JOURNAL OF SOLID STATE CHEMISTRY **84**, 71–81 (1990)

Solid State Carbon-13 and Proton NMR Studies of Carbonate-Containing Calcium Phosphates and Enamel

K. BESHAH,* C. REY†,[1] M. J. GLIMCHER,† M. SCHIMIZU,†,[2]
AND R. G. GRIFFIN*

**Francis Bitter National Magnet Laboratory, Massachusetts Institute of Technology, Cambridge, Massachusetts 02139; and †Harvard Medical School and Children Hospital, Boston, Massachusetts 02115*

Received June 1, 1989

Carbonate ions which replace phosphates—type B—and hydroxide ions—type A—in bone and synthetic apatites were studied by ^{13}C and ^{1}H solid state NMR spectroscopy. Heated apatites and dipolar suppression experiments have been employed to assign the spectra lines. Two overlapping peaks around 170 ppm which behaved differently on heating were assigned to type B carbontes. Pure type A carbonate gave a sharp signal at 166.5 ppm, and we were able to identify this signal in type AB apatite and in a presumably pure type B carbonate apatite. Amorphous calcium phosphate carbonates gave a broad gaussian peak of about 3 ppm at full width half-maximum with a center of gravity at about 168 ppm. The same resonance line, but with lower intensity, was also observed for apatites containing type A and B carbonates. Magic angle spinning ^{1}H NMR spectra of these apatites showed resolved OH^- and H_2O signals but were inconclusive in identifying specific structural and adsorbed H_2O groups. Implications of the NMR data to the crystal structure of carbonate apatites is discussed.

Introduction

The association of the CO_3^{2-} ions with apatites has been investigated by many different methods: X-ray diffraction (*1–5*), molar composition determinations (*4, 5*) infrared spectroscopy (*4–7*), Raman spectroscopy (*8*), electron spin resonance (*4, 9–11*), extended X-ray absorption fine structure (EXAFS) (*12*), and proton nuclear magnetic resonance (*13*). This profusion of techniques is representative of the complexity of the problem and of its importance. Carbonate is the third most abundant constituent of bone and tooth mineral after calcium and phosphate and has been shown to play an important part in the dissolution (*14, 15, 17*) of the mineral phase in several of the biological processes concerned with calcification (*16, 17*).

The general structure of carbonate-containing phosphates has generally been found to be apatitic; however, synthetic amorphous calcium phosphate carbonates have also been prepared (*18–20*). The apatites have two types of anionic sites: the

---

[1] Present address: Laboratoire de Physico Chemie des Solides, Toulouse, France.

[2] Present address: School of Dental Medicine, Tsurumi University, Yakohama, Japan.

monovalent ones which are located in channels along the *c*-axis of the hexagonal structure, and are generally occupied by hydroxide, chloride, or fluoride ions (*29*), and the trivalent ones in which the phosphate ions are located.

X-ray diffraction, infrared spectroscopy, and molecular formulae determinations show that the carbonate ion associated with apatites may be located in the two monovalent and trivalent positions named type A and type B carbonate sites, respectively (*1–7*). The charge balance due to these substitutions involves complex vacancy formations or cationic replacements (*1–5*).

In particular, the substitutions of PO_4^{3-} by CO_3^{2-} leaves an oxygen vacancy in the structure which has been shown to be possibly occupied by F^- in minerals such as francolite or synthetic compounds (*4, 22*). Similar associations of CO_3^{2-} with a hydroxide ion have been observed in carbonate hydroxyapatite. Therefore, several OH^- locations may also exist in carbonate apatites (*4*).

Type A and type B carbonate apatites have also been observed in enamel and bone (*6, 20*). However, the IR spectrum of enamel suggests other environments of the CO_3^{2-} as well (*24*). The aim of this study is to identify and characterize the possible environments of carbonate and hydroxide ions in synthetic apatites and certain biological apatites using high resolution ^{13}C and ^{1}H NMR techniques.

Materials and Methods

I. Sample Preparation

The type A carbonate apatite was prepared by high temperature treatment (900°) of a stoichiometric hydroxyapatite (*25*) in an atmosphere of $^{13}CO_2$ for 10 days (*2, 25*).

The amorphous calcium phosphate was prepared by double decomposition between a calcium nitrate solution and an ammonium phosphate solution containing CO_3^{2-} ions. The phosphate–carbonate solution [$(NH_4)_2$ HPO_4: 1 g; $NaH^{13}CO_3$: 0.2 g; ammonia solution: 5 ml; H_2O: 30 ml] was rapidly poured at room temperature into the calcium solution [$Ca(NO_3)_2 4H_2O$: 2.4 g; ammonia solution: 5 ml; H_2O: 100 ml]. The precipitate was immediately filtered, washed and lyophilized.

The mixed type A and type B carbonate apatites were obtained by thermal crystallization of the amorphous carbonate phosphate or by double decomposition. The thermal crystallization of amorphous carbonate phosphate at 500–600°C has been shown to produce an apatite containing the carbonate ion in the two anion sites (*19, 20*). Such formation gives rise to well crystallized apatites, provided the content in CO_3^{2-} of the initial amorphous compound is not too high (*19*). The amorphous calcium phosphate carbonate prepared as described above has been heated at 520°C in an open furnace for 1 hr. The conversion of these compounds to apatite was ascertained by X-ray diffraction and IR spectroscopy.

The aqueous preparation of carbonate apatite allows us to control more specifically the distribution of the carbonate ions between site A and site B (*4*) and their pattern of formation seems more closely related to that of biological apatites.

The pure type B apatite was prepared according to the method described by Labarthe *et al.* (*5*). The solution of phosphate and carbonate ions [$(NH_4)_2HPO_4$: 1 g; $Na_2{}^{13}CO_3$: 0.5 mg; ammonia solution (specific gravity: 0.90): 10 ml; H_2O: 30 ml] was added drop by drop to the calcium solution [$Ca(CH_3COO)_2$, 0.5 H_2O: 1.66 g; ammonia solution: 20 ml; H_2O: 100 ml] at 80°C in a closed atmosphere. Precipitation time was 3 hr. The precipitate was allowed to mature for 15 hr, then was filtered, washed with distilled water, and dried at 70°C.

The type AB apatite was obtained in less basic conditions (*4*) with a short maturation time. A solution with the same concentration of salt as that used to prepare type B apatite preparation was used but without addition of ammonia. Temperature was 80°C and precipitation time was 1 hr. Maturation time was 30 min and the termination was unchanged.

All samples were checked by X-ray diffraction. Except for the amorphous phosphates, they were of apatitic structure and did not contain any crystalline calcium carbonate. The carbonate location was ascertained by IR spectroscopy.

II. NMR Measurements

We have employed cross-polarization (CP) (*41*) and magic angle spinning (MAS) techniques to obtain the ^{13}C spectra of AB type carbonate-containing calcium phosphates on our home-built NMR spectrometer operating at 79.9 MHz for carbon and 317.7 MHz for protons. The CP experiment involves a single contact Hartman-Hahn matched condition and a proton decoupling power of greater than 60 kHz. Due to the absence of ^{13}C–^{1}H bonds in carbonates, the proton–carbon dipolar coupling is weak and long mixing times, about 10 msec, were required to achieve maximum polarization transfer. The proton NMR was performed at 397.7 MHz using the Bloch decay (single pulse) sequence. Spinning rates were 2 to 3.4 kHz for ^{13}C-NMR (in double-bearing ceramic rotors) and about 11 kHz for ^{1}H NMR (in double-drive 5-mm silicon nitride rotors) (Doty Scientific, Inc., Columbia, SC). All shifts are referenced to external tetramethylsilane (TMS).

The pulse sequences used to obtain the ^{13}C spectra were of three types: (i) Bloch decay experiment, with a recycle delay time of about 60 sec; (ii) normal cross polarization with a mixing time of 10 msec and a repetition time of 5 sec; (iii) in addition to the normal CP sequence, data acquisition and proton decoupling were delayed by one or two rotor periods (*42*). This delay allows the ^{13}C magnetization of those nuclei which are relatively close—more coupled—to protons to be dephased and the ^{13}C signal intensity will be suppressed. The technique assists in the identification of CO_3^{2-} close to H_2O.

Results

The ^{13}C CP–MAS NMR spectrum of carbonate-containing amorphous apatite is shown in Fig. 1A. The center band shown in the figure has a broad signal with its center of gravity at 169.5 ppm and a linewidth of about 3 ppm. Owing to its poor crystallinity, each CO_3^{2-} ion has a slightly different chemical environment, resulting in a distribution of isotropic chemical shifts which is characterized by the broad gaussian NMR signal.

Figure 1B shows the center band of the Bloch decay MAS–NMR spectrum of type A CO_3^{2-} apatite with a single isotropic line at 166.5 ppm. Its chemical shift anisotropy covers about 10 kHz range as determined from the rotational sidebands. CP experiments were not possible on type A apatite because CO_3^{2-} replaces ^{-}OH, depleting the main proton source for the polarization transfer.

The type B apatite gives an asymmetric signal (Fig. 1C), indicative of the presence of several CO_3^{2-} environments. The maximum of this peak was at 170.2 ppm, and a very small peak at 166.5 ppm indicates the presence of a small amount of type A carbonate which was not detected by IR spectroscopy.

The type AB apatite (Fig. 1D) exhibited, as expected, a spectrum characterized by a peak of low intensity corresponding to the type A carbonate and an intense peak at the position of the type B carbonate. In addition, a third peak appeared at 168.2 ppm which corresponded to the position of CO_3^{2-}

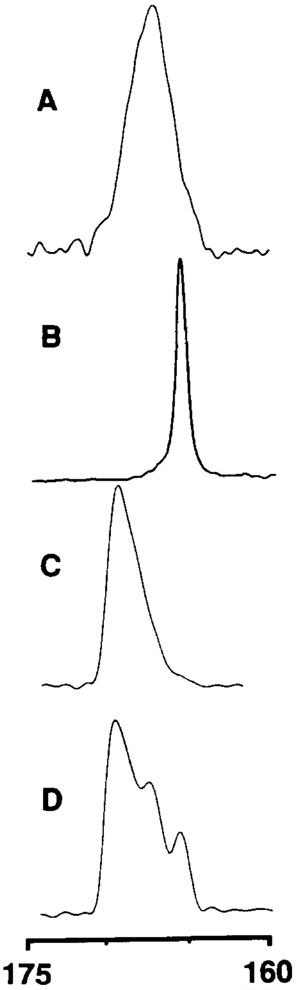

FIG. 1. ^{13}C MAS-NMR spectra of various CO_3^{2-} types present in synthetic calcium phosphates: (A) amorphous carbonate, (B) type A carbonate, (C) type B carbonate, and (D) type AB carbonate.

ions in amorphous carbonate phosphate. In order to better understand this asymmetric peak at 170.2 ppm of type B and type AB apatites, the samples were heated at 400°C and a dipolar suppression experiment carried out which allowed us to differentiate the carbonate species close to protons.

The spectra obtained after heating at 400°C for 24 hr show narrower linewidths for the type B carbonates which seem to be "shifted" upfield from 170.2 to 169.7 ppm. The "shifted" peak is within the broader linewidth of the unheated type B peak. In other words, heating does not create a new type B carbonate but rather favors one of the overlapped type B carbonates observed as asymmetric features at lower temperature. These data illustrate the existence of two type B CO_3^{2-} at moderate temperature.

Overall, the spectra in Fig. 2 showed that when the carbonate apatites are heated to 400°C better resolved signals are observed for the type B and type AB carbonates which are characteristic of higher crystallinity in the solid phase.

Moreover, the signal of the heated type AB apatite showed loss of intensity of its 168.2 ppm peak which is consistent with the assumption that the carbonate species responsible for this peak are in an unstable environment, possibly analogous to that of amorphous calcium carbonate phosphate. The decrease of this peak intensity as the reaction temperature increases could be due to the formation of more crystalline apatite from the perturbed fraction. As illustrated in Figs. 1 and 2, the relative intensity of the resonance line at about 168.2 ppm is very helpful in determining the amorphous-like or more unstable environment of carbonate in apatites. This evolution is consistent with that observed by infrared spectroscopy (*23*).

A dipolar suppression experiment on these samples did not change the type B apatite signal, while it suppressed the peak of the type AB apatite at 168.2 ppm, suggesting that the unstable carbonate is adjacent to protons. In order to obtain further information on this domain, type AB apatite, prepared by crystallization of the amorphous carbonate phosphate at 520°C, was examined by ^{13}C and ^{1}H NMR. A better resolved ^{13}C NMR spectra was ob-

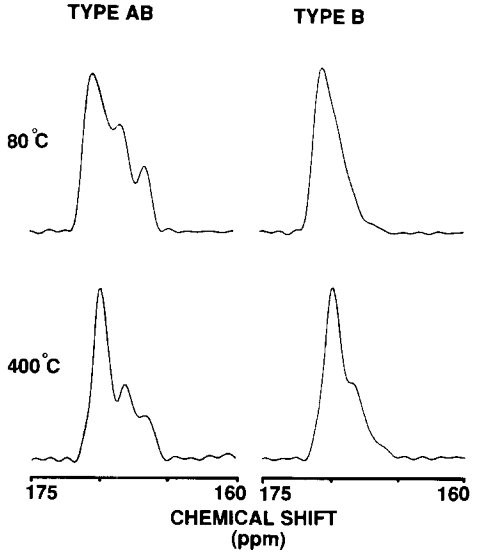

FIG. 2. ^{13}C CP–MAS NMR spectra of type AB (low $^{-}$OH and Ca/P ratio) and type B (high $^{-}$OH content and Ca/P ratio) apatites treated at the indicated temperatures. Note the better resolved peaks at higher temperature for both types and the relative loss in intensity of the middle peak at 168.2 ppm. See text for details.

tained from this sample as shown in Fig. 3A. The resolved signals are from magnetically inequivalent CO$_3^{2-}$ forms. Apart from the three distinctly resolved resonance lines, two shoulder signals are observed on the two most intense, downfield peaks.

Figure 3B shows a CP–MAS spectrum with delayed decoupling and acquisition which suppressed ^{13}C signals strongly coupled to protons. The middle resonance line at 168.4 ppm, which appears to correspond to the amorphous-like CO$_3^{2-}$ peak, is more affected than any of the other CO$_3^{2-}$ peaks, implying that it is closer to protons. Moreover, the multiplets are better resolved in the dipolar suppression spectrum of both type B and the amorphous-like peaks (Fig. 3B). In particular, its first derivative shown on the side clearly deconvolves the shoulder peaks.

One may conclude that at least five different carbonate environments may exist in apatites. The environment corresponding to the 168.2 ppm signal seems very different from the others: Its intensity decreases during heating at moderate temperatures and the corresponding carbonate species seem to be closer to protons. This environment is superimposed on another CO$_3^{2-}$ peak which appears to be less sensitive to suppression experiments, see Fig. 3. The most intense peak at 170.2 ppm may be considered as a superimposed peak corresponding to two important locations found in type B apatites. The NMR signal due to type A carbonate appears in all precipitated apatites, even in presumably "pure" type B apatite, according to their IR spectra.

Observation of carbonate ions in biological apatites is not possible because of in-

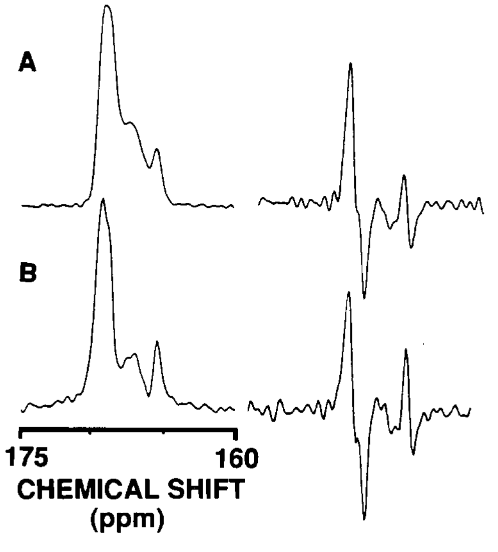

FIG. 3. Effect of delayed decoupling (B)—suppression experiment—on calcined (540°C) type AB apatite. Further special resolution is obtained by heat treatment owing to better crystallinity at higher temperature. Five resonance lines are identified which are better illustrated by the first derivatives on the right side of each spectrum. The amorphous-like peak at the middle (168.2 ppm) is suppressed indicating its proximity to protons.

tense bands due to the presence of natural abundance ^{13}C in the organic components of the bone matrix. Although reactions of bone with hydrazine are effective in deproteinizing this tissue *(26)*, the small residue of organic matrix which remains in the bone prevents a clear observation of the carbonate peaks. However, the ^{13}C-NMR spectra of dental enamel (96% mineral, 3.6% carbonte) exhibit a weak signal which can be unambiguously assigned to CO_3^{2-} ions.

As shown in Fig. 4, the major features of the synthetic apatite signals are reproduced. The resonance lines particularly at 170.5 ppm for the type B and at 166.9 ppm for the type A carbonates are very prominent. Although the limited signal-to-noise and resolution prevent assigning all resonance line(s), a comparison with the spectra of synthetic compounds clearly shows the presence of other carbonate locations. These results are consistent with those obtained by IR spectroscopy. It should be emphasized, however, that the amount of amorphous-type or unstable carbonate is very low in fully mineralized enamel *(40)*.

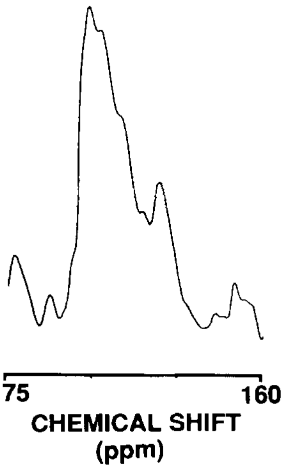

FIG. 4. ^{13}C CP–MAS spectrum of half-erupted enamel. Although the poor signal-to-noise does not enable us to properly resolve all the lines, the major features—type B and type A peaks—can be easily correlated to the synthetic apatites.

III. Proton NMR

The 168.2 ppm ^{13}C signal of apatites has been shown to correspond to a carbonate ion in close proximity to a proton. The existence of CO_3^{2-}—OH^- or CO_3^{2-}—H_2O complexes has been suggested in which the OH^- ion or the H_2O molecule may occupy the oxygen vacancy left by the substitution of PO_4^{3-} with CO_3^{2-} *(4)*. In order to identify such associations, a ^1H-NMR investigation was performed on type AB apatite rich in OH^- and type AB apatite containing only traces of this ion.

Figure 5 illustrates solid state ^1H NMR spectra of type B (5A) and type AB (5B) apatites with high and low calcium and hydroxyl content respectively and amorphous (5C) calcium phosphate. The spectra were obtained with a Bloch decay MAS experiment with ν_r = 11 kHz. The two prominent signals at −0.6 and 4.8 ppm (with respect to external TMS) are center bands while the remaining smaller periodic peaks are due to rotational sidebands. A comparison of the spectra in Fig. 5 with those obtained for brushite ($CaHPO_4 \cdot 2H_2O$) and hydroxyapatite $\{Ca_{10}(PO_4)6(OH)_2\}$ (not shown here) led to the assignment of the resonance line at −0.6 ppm to the ^-OH group and the 4.8 ppm peak to H_2O. The signal from amorphous phosphate is mainly from H_2O as expected because of the high water content (10% H_2O by weight).

This is one of the rare cases of highly resolved ^1H NMR spectra of polycrystalline solids obtained without homonuclear multiple pulse decoupling sequences. It was possible mainly because of the low ^-OH and H_2O concentrations which are widely separated from each other in the crystal lattice. Hence, the ^1H dipole–dipole

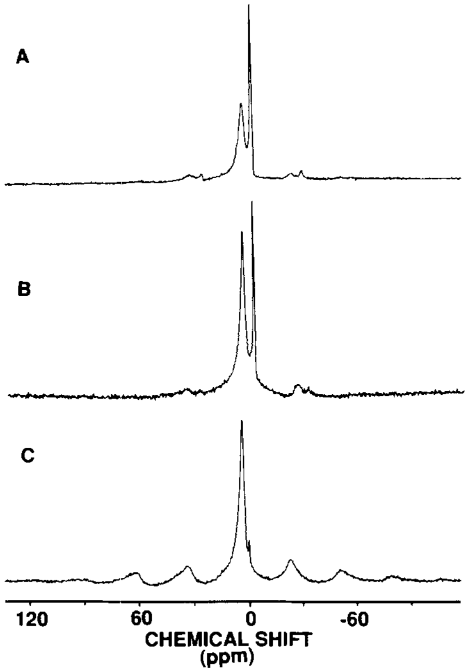

FIG. 5. ^{1}H MAS-NMR spectrum of (A) type B apatite, (B) type AB apatite, and (C) amorphous calcium phosphate. The spectra were obtained by one pulse experiments spinning speeds of about 11 kHz. The $^{-}$OH group signal is at −0.6 ppm and the H_2O peak is at 4.8 ppm. The smaller periodic peaks denoted by ss are spinning sidebands.

interaction is weak and enables the separation of $^{-}$OH and H_2O signals.

The nonspinning spectra of apatites (not shown) is dominated by the signal from H_2O which is essentially similar to the spinning spectrum without the $^{-}$OH peak and rotational sidebands. Even though the water signal exhibits sidebands with spinning experiments, the reasonably narrow (2.3 ppm at FWHM) nonspinning H_2O signal in amorphous apatite (Fig. 5C) illustrates the substantial mobility of the adsorbed water molecule. Our result could identify only one isotropic ^{1}H shift of H_2O in all types of apatites we studied. One cannot rule out the possibility of two or more structural or adsorbed H_2O forms that differ by the strength of binding to the crystal lattice. The part of the H_2O signal that gave the strong sidebands could be due to structural and/or strongly bound H_2O molecules while the narrow nonspinning portion could be due to weakly bound water molecules.

On the other hand, the $^{-}$OH NMR signal of apatites is so broad that it was not possible to detect it in such a small number of acquisitions (typically 100). With MAS, a sharp isotropic signal (1 ppm at FWHM) flanked by spinning sidebands was observed which is typical of crystalline solids. The relative ratio of $^{-}$OH and H_2O peaks clearly shows the $^{-}$OH content in each type of apatite. These ratios ascertain our synthesis of high and low hydroxyl-containing apatites. Only one $^{-}$OH group was apparent, suggesting the existence of a unique environment for this ion. However, other $^{-}$OH groups, such as one suggested to be associated with CO_3^{2-}, has been shown to be very low in concentration and another $^{-}$OH environment could remain undetected in samples rich in $^{-}$OH ions. ^{1}H NMR spectra obtained at higher field strength (*27*) and high spinning speeds may give sufficient dispersion of the signals to resolve additional lines in these systems.

Discussion

^{13}C solid state NMR techniques have enabled us to identify five magnetically inequivalent CO_3^{2-} ions in apatites. The difference in the chemical shift of the two widely recognized type A (~166.5 ppm) and type B (~170 ppm) carbonates may be due to differences in either their chemical environments or geometric factors. In the latter case, factors such as shorter bond lengths between carbon and oxygen could result in more shielding of the carbonate carbon or distortion of the planar structure, possibly rearranging the *p*-electrons in the bonding orbitals of the type A carbonate, resulting in an upfield shift of the ^{13}C resonance line. Such geometric factor effects on chemical shifts have been demonstrated in many instances (*43*, *44*). Moreover, this interpretation seems consistent with the IR spectra. The distortion of the CO_3^{2-} ion from the planar D_3h symmetry is related to the splitting of the ν_3 band (*28*) which appears stronger in the type A (80 cm^{-1}) than in the type B (40 cm^{-1}) carbonate location.

The carbonate species that gave rise to the NMR signal at 168.2 ppm exhibits a unique property due to its coupling with protons and its thermal instability. Several causes may be proposed for a strong coupling of a carbonate ion with protons. The hypothesis of a HCO_3^- ion can be ruled out: the NMR signal is still sensitive to suppression experiments after heating at 400°C and a bicarbonate ion would not be resistant to a 24-h period treatment at this temperature. For the same reason the association with a HPO_4^{2-} ion seems unlikely. The only heat-resistant protonated species in the apatitic structure is the OH^- ion. However, an association of CO_3^{2-}—OH^- still does not match the data: the 168.2 ppm signal is observed with the strongest intensity in the type AB apatites which contain only a small amount of hydroxide ions, barely observable on the IR spectra. It would appear that the most likely explanation for the presence of a proton associated to a carbonate ion in the type AB apatite is that there is an interaction with water molecules which could be reabsorbed on the sample after heating. Such an interpretation appears consistent with the ^1H NMR signal of the water molecule in these apatites shown in Fig. 5. The calcium phosphate with the most intense ^1H signal of H_2O also has the most intense ^{13}C signal of the amorphous-like carbonate at 168.2 ppm (Fig. 1A). Similarly, type B apatite has the least intense ^1H signal of H_2O (Fig. 5C) and ^{13}C signal of CO_3^{2-} at 168.2 ppm (Fig. 1C). Type AB apatite has intermediate intensity for water (Fig. 5B) and amorphous-like carbonate (Fig. 1D).

The decrease in intensity of this species during heating may evolve by at least three possible ways: (1) a decomposition of the unstable CO_3^{2-} species themselves; (2) the removal of water which can affect the efficiency of the CP experiment and therefore make this species indistinguishable from the others; (3) the increase in crystallinity and the progressive disappearance of these environments due to a restructuring of the crystal lattice. It seems probable that the development of an increase in crystallinity of the apatites is always being associated with an irreversible loss of water (*4*, *19*).

The apatitic structure appears as the only crystalline phase in the samples which we studied, and the existence of an amorphous carbonate phosphate seems unlikely, considering our conditions of preparation. Nevertheless, the "amorphous-like" carbonate species detected by NMR as well as by IR spectroscopy (*23*) exhibit properties which are very different from any of the other carbonate species which occupy well defined sites in the structure: they appear to be unstable on heating, easily accessible, and loosely bound to H_2O molecules. These features suggest a location on the surface of the crystals or in perturbed areas inside the crystals (*29–33*). Such locations have been postulated in biological as well as in synthetic apatites. They could be responsible for various phenomena such as anomaly of dissolution (*29*, *30*), trapping of CO_2 molecules during decomposition (*34*), surface radical formation after irradiation (*10*, *11*), or fast mineral mobilization from bone tissues (*17*). Very little is known about the environment of such ions except that it contains water molecules.

The other carbonate locations appear to be quite stable. The apatitic structure provides only two ionic sites and interstitial locations of bulky ions such as CO_3^{2-} can be excluded.

The carbonate ion in PO_4^{3-} site (type B) may occupy three nonequivalent crystallographical positions related to the occupancy of the four tetrahedral oxygen sites labeled I, II, III, III′ as shown in Fig. 6. As III and III′ are equivalent, the possible locations of the oxygen atoms of the CO_3^{2-} ion are I, II, III or I, III, III′ or II, III, III′. However, two of these positions—I, III, III′ and II, III, III′—are very similar and probably will not introduce significant differences in the NMR chemical shift or the IR carbonate band position. Polarized IR spectroscopy studies of oriented sections of enamel (*6*) suggest that the pseudoplanar CO_3^{2-} ion is tilted with respect to the *c*-axis and, therefore, its oxygen occupies the I, II, III (or III′) oxygen sites, the III′ (or III) site being vacant (Fig. 6) (*35*). Such data are unavailable for synthetic apatites and in this case the existence of another orientation of a CO_3^{2-}—[ ]o ion cannot be ruled out. Other kinds of type B carbonates may occur when the oxygen vacancy is occupied by a OH^- ion or H_2O as suggested by Vignoles (*6*). However, there is no evidence of such environments from ^{13}C- or ^{1}H-NMR studies.

Although evidence for the existence of several different kinds of type A carbonate positions has been presented by Vignoles (*6*), detailed descriptions of their characteristics are not yet available. The A sites are located in channels running along the *c*-axis of the apatitic structure (*21*). The location of the anions in the channel is not well defined and it may vary along the *c*-axis owing to the nature of the ion or the stoichiometry (*21*, *36*). Bulky ions seem to occupy a position near the distorted hexagon of

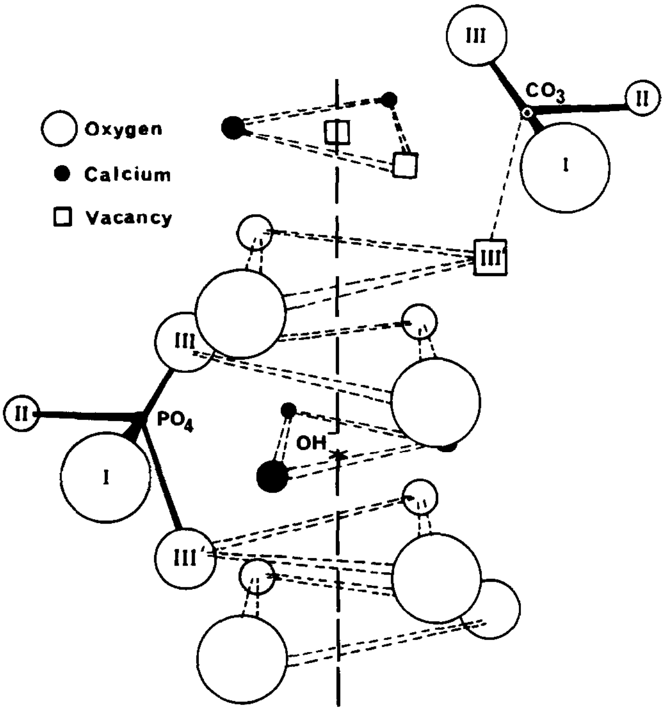

FIG. 6. Crystallographic position of type B carbonate apatite showing the four tetrhedral phosphate oxygen sites—I, II, III, III′—occupied by the three oxygens of the CO_3^{2-} ion. The one oxygen site left vacant is probably one of the reasons for the multiplet/broad type B ^{13}C signal observed.

oxygen atoms at $c/2$ which corresponds to the largest space in the channels (*37*).

There exists a single position for the carbonate ion in type A only carbonate apatite. It has been shown to interact strongly with phosphate ions, producing a distortion observable by IR on the $\nu 3$ PO_4^{3-} band (*38*) and by ^{31}P-NMR (*39*). In mixed AB apatites the replacement of PO_4^{3-} by CO_3^{2-} and a vacancy which seems to be located in the gauche hexagon (*35*) may modify the type A CO_3^{2-} environment. In addition, when types A and B are in direct interaction, a perturbation of the B carbonate analogous to that observed for PO_4^{3-} ions may occur.

It appears that several possibilities are provided for the environment of minor carbonate species. As the complexity of the IR and NMR spectra increases when the two species are simultaneously present, one may conclude that interactions between type A and type B carbonates, such as those depicted above, can be a cause for the existence of several kinds of environment. However, further work is needed to present a precise assignment for these resonance lines.

Acknowledgments

We thank Valerie Copié for help with the NMR experiments. This work was supported by grants from Orthopedic Research and Education Foundation Bristol-Myers Zimmer Corporation Institutional Grant, Program Project Grant (AR34078), Peabody Grant, and the Mineral Grant (AR34081).

References

1. R. Z. LEGEROS, Ph.D. thesis, New York University (1967).

2. G. BONEL, *Ann. Chim.* **7,** 65 (1972).

3. J. C. ELLIOTT, G. BONEL, AND J. C. TROMBE, *J. Appl. Crystallogr.* **13,** 618 (1980).

4. M. VIGNOLES, These d'Etat, Institut National Polytechnique de Toulouse (1984).

5. J. C. LABARTHE, G. BONEL, AND G. MONTEL, *Ann. Chim.* **8,** 289 (1973).

6. J. C. ELLIOTT, Ph.D. thesis, University of London (1964).

7. D. G. A. NELSON AND J. D. R. FEATHERSTONE, *Calcif. Tissue Int.* **34,** 69 (1984).

8. D. G. A. NELSON AND B. E. WILLIAMSON, *Aust. J. Chem.* **35,** 715 (1982).

9. H. J. TOCHON-DANGUY, M. GEOFFROY, AND C. A. BAUD, *Arch. Oral. Biol.* **25,** 357 (1980).

10. R. A. PEKAUSKAS AND I. PULLMAN, *Calcif. Tissue Res.* **25,** 37 (1978).

11. Y. DOI, Y. MORIWAKI, T. AOBA, J. TAKAHASHI, AND K. JOSHIN, *Calc. Tissue Int.* **34,** 178 (1982).

12. S. S. HASNAIN, *Springer Proc. Phys.* **2,** 145 (1984).

13. A. S. RAO AND K. S. MANJA, *Indian J. Pure Appl. Phys.* **15**(8), 565 (1977).

14. M. OKAZAKI, Y. MORIWAKI, T. AOBA, Y. DOI, AND J. TAKAHASHI, *Caries Res.* **15**(6), 471 (1981).

15. R. Z. LEGEROS AND M. S. TUNG, *Caries Res.* **17**(5), 419 (1983).

16. A. S. HALLWORTH, J. A. WEATHERELL, AND B. ROBINSON, *Caries Res.* **7,** 345 (1965).

17. R. M. BILTZ AND E. D. PELLEGRINO, *Mineral Electrolyte Metab.* **5,** 1 (1981).

18. G. MONTEL, These d'Etat, Faculte des Science de Paris (1958).

19. HEUGHEBAERT, These d'Etat, Institut National Polytechnique de Toulouse (1977).

20. J. D. TERMINE AND D. R. LUNDY, *Calcif. Tissue Res.* **13,** 73 (1973).

21. R. A. YOUNG, *J. Dental Res.* **53,** 193 (1974).

22. J. P. SMITH AND J. R. LEHR, *J. Agri. Food Chem.* **14,** 342 (1966).

23. C. REY, B. COLLINS, T. GOEHL, AND M. J. GLIMCHER, to be published.

24. J. C. ELLIOT, A. W. HOLCOMB, AND R. A. YOUNG, *Calcif. Tissue Int.* **37,** 372 (1985).

25. J. C. TROMBE, *Ann. Chim.* **8**(4), 251 (1973).

26. J. D. TERMINE, E. D. EANES, D. J. GREENFIELD, AND M. U. NYLEN, *Calcif. Tissue Res.* **12,** 73 (1973).

27. J. ARENDS, J. CHRISTOFFERSEN, H. ECKERT, B. O. FOWLER, J. C. HEUGEBAERT, G. H. NANCOLLAS, J. P. YESINOWSKI, AND S. T. ZAWACKI, *J. Cryst. Growth* **84,** 515 (1987).

28. Mineralogical Soc., "The Infrared Spectra of Minerals" (V. C. Farmer, Ed.), London (1974).

29. J. ARENDS AND W. L. JONGEBLOED, *J. R. Neth. Chem. Soc.* **100**(1), 3 (1981).

30. P. GARNIER, J. C. VOEGEL, AND R. M. FRANK, *J. Biol. Buccale* **4**(4), 323 (1976).

31. D. NELSON, *J. Dental Res.* **60,** 1621 (1981).

32. H. NAKAHARA AND M. KAKEI, "Tooth Enamel IV" (R. W. Fearnhead and S. Sugas, Eds.) (1984).

33. W. F. NEUMAN AND B. J. MULRYAN, *Calcif. Tissue Res.* **1,** 94 (1967).

34. S. E. DOWKER AND J. C. ELLIOT, *J. Solid State Chem.* **47**(2), 164 (1983).

35. G. BONEL AND J. C. LABARTHE, *Coll. Int. CNRS Paris,* 118 (1973).

36. A. J. C. WILLSON, K. SUDARSANAN, AND R. A. YOUNG, *Acta. Crystallogr. Sect. B* **33,** 3142 (1977).

37. C. REY, These d'Etat, Institute National Polytechniques de Toulouse (1984).

38. J. C. TROMBE AND G. MONTEL, *C. R. Acad. Sci. Paris* **276,** 1271 (1973).

39. R. AUE, A. H. ROUFOSSE, J. E. ROBERTS, M. J. GLIMCHER, AND R. G. GRIFFIN, *Biochem.* **23**(25), 6110 (1984).

40. C. REY, to be published.

41. A. PINES, M. J. GIBBY, AND J. S. WAUGH, *J. Chem. Phys.* **59,** 569 (1973).

42. S. J. OPELLA AND M. H. FREY, *J. Amer. Chem. Soc.* **101,** 5854 (1979).

43. R. RADEGLIA AND G. ENGELHARDT, *Chem. Phys. Lett.* **114,** 28 (1988).

44. S. RAMADAS AND J. KLINOWSKI, *Nature (London)* **308,** 521 (1984).